Hindawi Publishing Corporation
Mathematical Problems in Engineering
Volume 2016, Article ID 5898209, 10 pages
http://dx.doi.org/10.1155/2016/5898209

Research Article

A Control Method to Balance the Efficiency and Reliability of a Time-Delayed Pump-Valve System

Zhounian Lai,[1,2] Peng Wu,[1,2] Shuai Yang,[1,2] and Dazhuan Wu[1,2,3]

[1] *Institute of Process Equipment, Zhejiang University, Hangzhou 310027, China*
[2] *College of Chemical and Biological Engineering, Zhejiang University, Hangzhou 310027, China*
[3] *State Key Laboratory of Fluid Power and Mechatronic Systems, Zhejiang University, Hangzhou 310027, China*

Correspondence should be addressed to Dazhuan Wu; wudazhuan@zju.edu.cn

Received 26 May 2016; Revised 8 August 2016; Accepted 30 August 2016

Academic Editor: Olfa Boubaker

The efficiency and reliability of pumps are highly related to their operation conditions. The concept of the optimization pump operation conditions is to adjust the operation point of the pump to obtain higher reliability at the cost of lower system efficiency using a joint regulation of valve and frequency convertor. This paper realizes the control of the fluid conveying system based on the optimization results. The system is a nonlinear Multi-Input Multioutput (MIMO) system with time delays. In this paper, the time delays are separated from the system. The delay-free system is linearized using input-output linearization and controlled using a sliding mode method. A modified Smith predictor is used to compensate time delays of the system. The control strategy is validated to be effective on the test bench. The comparison of energy consumption and operation point deviation between conventional speed regulation and the new method is presented.

1. Introduction

As a key component of fluid conveying systems, pumps are widely used in industries, of which 45% are centrifugal pumps [1]. Pumps account for nearly 20% of electrical energy consumption and are in the range of 25%~50% of energy consumption in many industries [2]. Therefore energy saving in pumps is one main goal in industries, which requires pumps work in good operation points. Bad operation point leads to a low efficiency and reliability of a pump, causing serious consequences.

Many researchers focused on the energy saving of pump systems. The variable speed pump technology is widely used to reduce energy cost in industries. It varies the rotational speed of centrifugal pumps to accommodate pipeline requirements [3]. According to surveys and researches [4, 5], speed regulation can save 5%~50% energy relative to valve regulation. In recent years, the scheduling of pumps has progressed greatly. Wang et al. [6] proposed an enhanced genetic algorithm for pump scheduling in water supply system to reduce the energy cost and slow land subsidence. Hashemi et al. [7] developed an ant-colony optimization of pumping schedule using variable speed pumps and saved about 10% energy cost compared to single speed pumps. However, few studies on the pump reliability have been conducted so far.

Efficiency and reliability of a centrifugal pump are related to operation point of the pump. Efficiency of a centrifugal pump reaches its peak value at its design point and decreases as its operation point deviates from its design point [8]. Barringer [9] found out that reliability curve is similar to its efficiency curve. Reliability of a pump is a statistics term, which is defined as the mean time between failure (MTBF) relative to the mission time. Reliability of a centrifugal pump reaches a peak value at the Best Efficiency Point (BEP), near its design point, but decreases sharply as operation point deviates from design point, shown in Figure 1. Thus the operation point plays a decisive role in pump reliability. Long operating time at part load or overload may increase the component failure rate. High temperature rise, suction recirculation, and discharge recirculation may occur in a pump operating at part load, while low sealing life, low

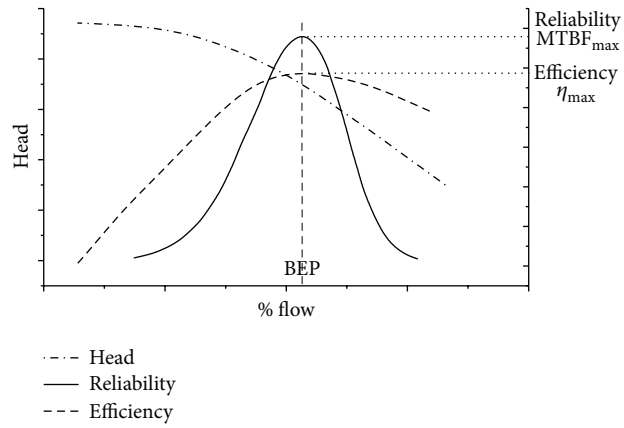

Figure 1: Reliability curve, efficiency curve, and head curve of a centrifugal pump.

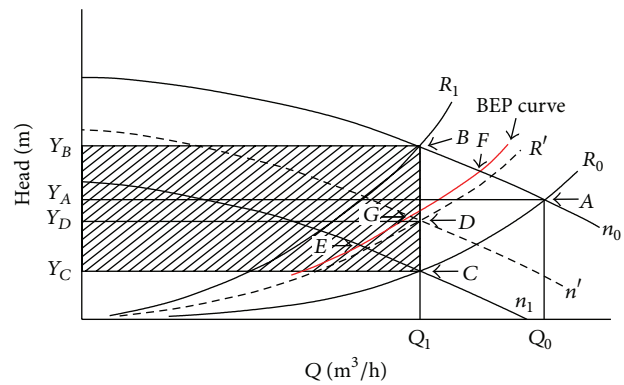

Figure 2: Comparison of valve regulation and speed regulation.

bear life, and cavitation may occur in a pump operating at overload, leading to a poor pump efficiency and reliability.

In our previous work [10], we developed an optimization algorithm to improve centrifugal pump reliability and efficiency for pump systems at the cost of a decline in system efficiency, using throttling valves and a pump number selection strategy to restrict the pump operation point to a neighbourhood of BEP. Compared with conventional speed regulation, one of the key concepts of our previous work [10] is to use a frequency converter to enlarge the BEP to a larger flow rate point and use a valve to enlarge pipeline characteristics to a certain point; therefore the operation point of the pump is limited to the BEP at the cost of increasing energy consumption at the valve. The genetic algorithm in our previous work [10] will calculate the pressure loss across the valve. However, the flow rate and the pressure loss across the valve are coupled, making it difficult to control these two variables simultaneously. In our previous work [10], the author was concerned with the allocation of flow rate and the pressure loss at the valve but did not mention the way to reach the desired flow rate and pressure loss.

Figure 2 shows a comparison of valve regulation, speed regulation, and the new method in our previous work [10] for a typical pump-valve system, where the x-axis is the flow rate Q and the y-axis is the head Y. Supposing the flow rate of the system is to regulate from Q_0 to Q_1, valve regulation changes pipeline characteristics from curve R_0 to R_1, resulting in a change of operation point from A to B, while speed regulation changes pump characteristics from curve n_0 to n_1, causing the operation point to change from A to C. It is clear that valve regulation causes a surplus head $(Y_B - Y_C)$ and thus leads to a significant energy waste, appearing as the shadowed area in Figure 2. Therefore substituting throttling valve regulations with speed regulations has become a widespread energy saving method [11]. In the case of conventional speed regulation in Figure 2, the Best Efficiency Point of speed regulation might be located at somewhere (point E) left of the operation point C; therefore the pump is operating at high flow rate point. Compared with conventional speed regulation, one of the key concepts of Wu's method [10] is to use a frequency converter to enlarge the BEP to a larger flow rate point D and use a valve to change pipeline characteristics to R'; therefore the operation point of the pump is limited to the BEP D at the cost of increasing energy consumption at the valve. The genetic algorithm in our previous work [10] will calculate the pressure loss across the valve. However, the flow rate and the pressure loss across the valve are coupled, making it difficult to control these two variables simultaneously.

This paper is an inherited work of our previous work [10] and aims at achieving the control of the two variables, flow rate and pressure loss across the valve of the pump-valve system, based on the optimization result of our previous work [10]. To emphasize the impact of valve on the pump operation point, this paper focuses on a one-pump system and gets rid of pump number selection strategy in our previous work [10]. This one-pump system is a special case of the multipump system in our previous work [10], because it can be regarded as small flow rate situation when only one pump is put into operation. The controlled variables of the pump-valve system are flow rate and the pressure loss across the valve, and the control variables are the pump speed and the valve lift. Since there are time delays in the valve actuator and the flow rate sensor, the pump-valve system is a nonlinear Multi-Input Multioutput (MIMO) system with time delays.

Many progresses have been made in the study of nonlinear MIMO systems during the past half century. The nonlinear MIMO systems with precise model are developed using input-output linearization to convert the nonlinear system into an equivalent linear systems in [12–14]. The nonlinear system with modelling imprecisions is presented using sliding model control in [13, 14] and adaptive control in [14]. As a simple approach to robust control, the sliding mode control for nonlinear systems with modelling imprecisions is implemented in a wide range of applications, such as electrohydraulic servo-mechanism [15, 16], electric drives [17], mechanical systems [18], and rigid manipulators [19]. During the past two decades, many approaches for uncertain nonlinear MIMO systems have been published. Shaocheng et al. [20] proposed a fuzzy adaptive indirect control for nonlinear MIMO systems with uncertainties using H_∞ tracking theory. The disturbances and fuzzy approximation errors are attenuated by a robust compensator to guarantee the

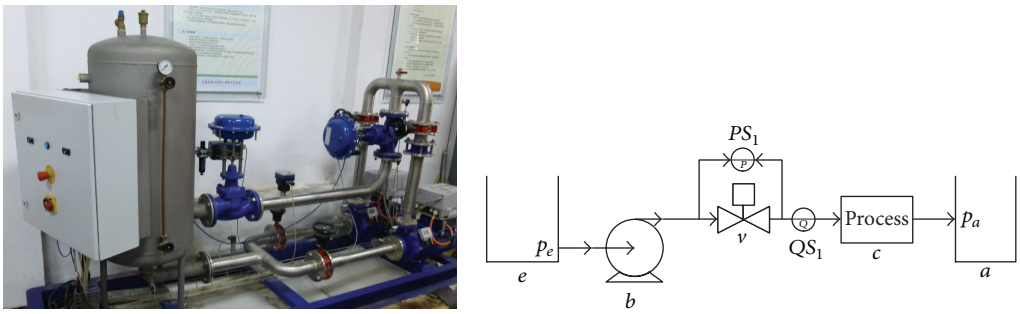

(a) Photograph of the test bench (b) Schematic of the test bench

Figure 3: Test bench.

robustness. Lin and Chen [21] developed a fuzzy sliding mode control for the nonlinear MIMO systems with uncertainties. Ge and Tee [22] and Chen et al. [23] proposed fuzzy adaptive method for nonlinear MIMO system with time delays. However, the complexity and the model restrictions of fuzzy adaptive method may limit their industrial applications.

The time delays of control systems are commonly balanced by Smith predictor which is used in many applications, such as water distribution system [24] and jet engine fuel controls [25]. Many modified Smith predictors have been put into application such as filtered Smith predictor [26].

In this paper, the time delays of the pump-valve system are isolated from the system, dividing the system into a delay-free system and a time-delay module. The delay-free system is controlled by a sliding mode controller while the time delays are compensated by a modified Smith predictor. This method takes full advantage of the existing imprecise system model and greatly decreases the complexity of the control algorithm compared to fuzzy adaptive method. In Section 2, a test bench composed of one pump and one valve is presented and modelled in state space model. In Section 3, the delay-free system is controlled by a sliding mode controller and the time delays are compensated by a modified Smith predictor. Section 4 presents the simulation result of the controller. The optimization strategy in our previous work [10] and the control strategy in Section 3 are combined and applied on the one-pump system and compared with conventional speed regulation.

2. System Model

A typical fluid conveying system test bench is built. The bench consists of two parallel installed centrifugal pumps (Etanorm 32–160, rated flow $25\,\mathrm{m}^3/\mathrm{h}$ and rated speed 2950 rpm, equipped with a frequency convertor) with manual valves installed at both ends of each pump, two pneumatic control valves (BOA-CVP H), and a water tank. As previously described, only one pump is applied in this paper; the other pump will not be used. The fluid in this study is chosen as water due to easy access and low costs. Water flows from the tank and flows back to the tank after a circulation though the centrifugal pump and the valves. Therefore the test bench can be described as Figures 3(a) and 3(b), where b denotes the centrifugal pump, v denotes the pneumatic control valve, c denotes a typical pressure load (represented by the other pneumatic control valve), PS_1 denotes the pressure sensor that measures the pressure difference across the valve, QS_1 denotes the flow sensor, and e/a denotes the tank.

The mathematical model of the system can be developed by applying Bernoulli's principle [27] at entry e and exit a, as shown in

$$\rho g z_e + P_e + \frac{\rho}{2} v_e^2 = \rho g z_a + P_a + \frac{\rho}{2} v_a^2 + \rho \int_e^a \frac{\partial v(l,t)}{\partial t} \partial l + \rho g h_f, \tag{1}$$

where g denotes the gravitational acceleration, z denotes vertical height, v denotes flow velocity, ρ denotes fluid density, P denotes fluid pressure, t denotes time, h_f denotes the friction head, and l denotes the location along streamline coordinate. The diameter of pipes is constant and the water is considered to be incompressible since the compressibility of liquid is very low [27]; therefore the flow velocity is independent of the streamline coordinate. Therefore the inertia term in (1) can be simplified to (2) according to [27]

$$\rho \int_e^a \frac{\partial v(l,t)}{\partial t} \partial l = \frac{\rho L}{A} \dot{Q}, \tag{2}$$

where L denotes the length of the pipe between entry e and exit a; A denotes the cross-sectional area of the pipe; Q denotes the flow rate in the pipe; and the overdot denotes its time derivative. The friction term $\rho g h_f$ can be considered as a sum of pressure loss ΔP (valve v) and ΔP_c (process load) as well as pressure source ΔP_p (pump b); (1) yields to

$$\rho g (z_a - z_e) + P_a - P_e + \frac{\rho}{2}\left(v_a^2 - v_e^2\right) = -\frac{\rho L}{A}\dot{Q} + \Delta P_p - \Delta P - \Delta P_c. \tag{3}$$

Since the entry e and the exit a are the same tank with small difference in vertical height, therefore it is reasonable

to assume $z_a = z_e$, $P_a = P_e$, and $v_a = v_e$. Ultimately, (1) can be written as fluid dynamic equation (4) as follows:

$$\dot{Q} = \frac{A}{\rho L}\left[\Delta P_p - \Delta P - \Delta P_c\right]. \tag{4}$$

The pump performance at rated speed n_r is a quadratic polynomial of flow rate and $\Delta P_{pn_r} = d_1' Q_{n_r}^2 + d_2' Q_{n_r} + d_3'$, which can be expanded to (6) at any given speed n by applying pump similarity law equation (5) [8]. The pressure loss ΔP (valve v) is relevant to installation conditions, fluid type, flow rate Q, and flow coefficient $K(H)$, where H denotes valve lift. In this paper, the fluid is water and the valve is standardly installed, which yields (7) [28], where $\Delta P_{\text{ref}} = 1 \times 10^5$ Pa. The pressure loss of ΔP_c (process load) is quadratic to flow rate [8], as shown in (8) as follows:

$$\frac{Q}{Q_{n_r}} = \frac{n}{n_r}, \qquad \frac{\Delta P_p}{\Delta P_{pn_r}} = \left(\frac{n}{n_r}\right)^2, \tag{5}$$

$$\begin{aligned}\Delta P_p &= d_1'\left(\frac{n}{n_r}\right)^2 + d_2'\left(\frac{n}{n_r}\right)Q + d_3' Q^2 \\ &\triangleq d_1 n^2 + d_2 n Q + d_3 Q^2,\end{aligned} \tag{6}$$

$$\Delta P = \frac{Q^2}{K^2(H)}\Delta P_{\text{ref}}, \tag{7}$$

$$\Delta P_c = K_c Q^2, \tag{8}$$

where d_1', d_2', d_3', d_1, d_2, and d_3 are the pump parameters; n denotes speed of the pump; K_c denotes the resistance coefficient of the process load c. The dynamic response of the pneumatic valve and the frequency convertor can be described as first-order linear systems [29, 30], as shown in

$$\dot{H} = \frac{1}{T_H}\left(H_{\text{set}} - H\right), \qquad \dot{n} = \frac{1}{T_n}\left(n_{\text{set}} - n\right), \tag{9}$$

where T_H and T_n are the time constant of valve actuator and frequency converter and H_{set} and n_{set} denote the set values of H and n. According to the aims of the controller, the controlled variables are chosen to be flow rate requirement Q_{set} and pressure loss ΔP_{set}. The pressure loss across the valve ΔP_{set} equals the difference of pump head and system required head by the genetic algorithm in our previous work [10]. By applying (6), (7), and (8) to (4) and combining with (9), a state space model of the plant can be derived. The overall state space model can be described by (10). The system is a nonlinear MIMO system, whose time delays are omitted in (10) due to a comprehensible description:

$$\dot{x} = f(x) + g(x)u, \qquad y = h(x), \tag{10}$$

where

$$x = \left[x_1 \;\; x_2 \;\; x_3\right]^T = \left[Q \;\; H \;\; n\right]^T, \tag{11}$$

$$f(x) = \begin{bmatrix} \frac{A}{\rho L}\left[d_1 n^2 + d_2 n Q + \left(d_3 - \frac{\Delta P_{\text{ref}}}{K^2(H)} - K_c\right)Q^2\right] \\ -\frac{1}{T_H}H \\ -\frac{1}{T_n}n \end{bmatrix} \triangleq \begin{bmatrix} w_1 \\ -\frac{1}{T_H}H \\ -\frac{1}{T_n}n \end{bmatrix}, \tag{12}$$

$$g(x) = \left(g_1 \;\; g_2\right) = \begin{pmatrix} 0 & 0 \\ \frac{1}{T_H} & 0 \\ 0 & \frac{1}{T_n} \end{pmatrix}, \tag{13}$$

$$u = \left[u_1 \;\; u_2\right]^T = \left[H_{\text{set}} \;\; n_{\text{set}}\right]^T, \tag{14}$$

$$y = \left[Q \;\; \Delta P\right]^T, \tag{15}$$

$$h(x) = \left[Q \;\; \frac{\Delta P_{\text{ref}}}{K^2(H)}Q^2\right]^T, \tag{16}$$

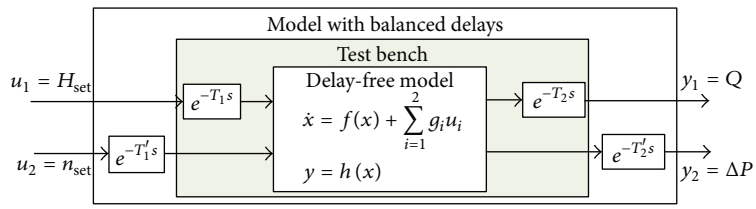

Figure 4: Test bench model, delay-free model, and model with balanced delays.

$$\begin{aligned}
&\left(g_1 \;\; g_2 \;\; ad_f g_1 \;\; ad_f g_2 \;\; ad_f^2 g_1 \;\; ad_f^2 g_2\right) \\
&= \begin{pmatrix} 0 & 0 & -\frac{1}{T_H}\frac{\partial w_1}{\partial Q} & -\frac{1}{T_n}\frac{\partial w_1}{\partial n} & \left(-\frac{1}{{T_H}^2}+\frac{1}{T_H T_n}\right)\frac{\partial w_1}{\partial H} & \left(-\frac{1}{{T_n}^2}+\frac{1}{T_H T_n}\right)\frac{\partial w_1}{\partial n} \\ \frac{1}{T_H} & 0 & \frac{1}{{T_H}^2} & 0 & \frac{1}{{T_H}^3} & 0 \\ 0 & \frac{1}{T_n} & 0 & \frac{1}{{T_n}^2} & 0 & \frac{1}{{T_n}^3} \end{pmatrix}.
\end{aligned} \tag{17}$$

As to the real test bench, time delays are observed in the valve actuator and the flow sensor. The time delays cannot be neglected due to the connection with system dynamics. The inputs and outputs of the system can be observed visually from the system model in Figure 4, where T_1 denotes time delay of the valve actuator and T_2 denotes time delay of the flow sensor. Since the actuators and the sensors of the systems have different delays, virtual delays $T_1' = T_1$ and $T_2' = T_2$ are added to the other input-output channels to balance the delays and obtain a synchronization performance of the system outputs.

3. Controller Design

Considering the pump-valve system is a time-delay system, we isolate the time delays of the system. The system without delays is controlled by a sliding mode controller and the time delays are compensated by a modified Smith predictor.

3.1. Control the Delay-Free Model. By applying Lie-derivative to the delay-free system equation (10), it is simple to linearize the input-output as

$$\begin{bmatrix} y_1^{(r_1)} \\ y_2^{(r_2)} \end{bmatrix} = \begin{bmatrix} y_1^{(2)} \\ y_2^{(1)} \end{bmatrix} = F + G \begin{bmatrix} u_1 \\ u_2 \end{bmatrix}, \tag{18}$$

where r_1 and r_2 are the relative degrees of the system, $r_1 = 2$ and $r_2 = 1$, respectively.

$$\begin{aligned}
F &= \begin{bmatrix} L_f^2 h_1(x) \\ L_f h_2(x) \end{bmatrix} \\
&= \begin{bmatrix} w_1 \frac{\partial w_1}{\partial Q} - \frac{1}{T_H} H \frac{\partial w_1}{\partial H} - \frac{1}{T_n} n \frac{\partial w_1}{\partial n} \\ w_1 \frac{2\Delta P_{\text{ref}} Q}{K^2(H)} + \frac{2\Delta P_{\text{ref}} Q^2}{T_H K^3(H)} \frac{\mathrm{d}K(H)}{\mathrm{d}H} \end{bmatrix} \triangleq \begin{bmatrix} f_1 \\ f_2 \end{bmatrix},
\end{aligned} \tag{19}$$

$$\begin{aligned}
G &= \begin{pmatrix} L_{g_1} L_f h_1(x) & L_{g_2} L_f h_1(x) \\ L_{g_1} h_2(x) & L_{g_2} h_2(x) \end{pmatrix} \\
&= \begin{pmatrix} -\frac{2A\Delta P_{\text{ref}} Q^2}{\rho L T_H K^3(H)} \frac{\mathrm{d}K(H)}{\mathrm{d}H} & \frac{A}{\rho L T_n}(2d_1 n + d_2 Q) \\ -\frac{2\Delta P_{\text{ref}} Q^2}{T_H K^3(H)} \frac{\mathrm{d}K(H)}{\mathrm{d}H} & 0 \end{pmatrix} \\
&\triangleq \begin{pmatrix} g_{11} & g_{12} \\ g_{21} & g_{22} \end{pmatrix}.
\end{aligned} \tag{20}$$

The singularity of G should be validated. The valve flow coefficient $K(H)$ is monotonically decreasing with valve lift H [28]; therefore its derivative is negative. The pump parameters d_1 and d_2 are positive; therefore G is nonsingular and invertible. By applying Lie bracket to (10), the controllability matrix can be obtained as (17). It has rank 3; therefore the system is controllable [31].

The r_ith derivative of output y_i is linearly related to the inputs u. By controlling the r_ith derivative of output y_i, the control of the output y_i is achieved. The model described by (10) in this paper yields to two decoupled single-input-single-output systems, one two-order (relative degree $r_1 = 2$) system for flow rate Q and one one-order (relative degree $r_2 = 1$) system for pressure loss across the control valve. It is easier to implement decoupling controller on the linear MIMO system. Since $r_1 = 2$ and $r_2 = 1$, the total relative degree equals the number of states; therefore the system will have no internal dynamics [14] and all the states of the system are observable.

In order to track target signal y_{di}, define a sliding surface $s_i = 0$ as (21), where $e_1 = y_{d1} - y_1$ and $e_2 = y_{d2} - y_2$ are the tracking errors of outputs.

$$S = \begin{bmatrix} s_1 \\ s_2 \end{bmatrix} = \begin{bmatrix} e_1^{(r_1-1)} + \alpha_{1(r_1-1)} e_1^{(r_1-2)} + \cdots + \alpha_{11} e_1 \\ e_2^{(r_2-1)} + \alpha_{2(r_2-1)} e_2^{(r_2-2)} + \cdots + \alpha_{21} e_2 \end{bmatrix}$$

$$= \begin{bmatrix} \dot{e}_1 + \alpha_{11} e_1 \\ e_2 \end{bmatrix}. \tag{21}$$

Combining (18), the derivative of s_i can be written as

$$\dot{S} = \begin{bmatrix} \dot{s}_1 \\ \dot{s}_2 \end{bmatrix} = \left(\begin{pmatrix} m_1 \\ m_2 \end{pmatrix} - F - Gu \right), \tag{22}$$

where

$$\begin{aligned} \begin{pmatrix} m_1 \\ m_2 \end{pmatrix} &= \begin{pmatrix} y_{d1}^{(r_1)} + \alpha_{1(r_1-1)} e_1^{(r_1-1)} + \cdots + \alpha_{11} \dot{e}_1 \\ y_{d2}^{(r_2)} + \alpha_{1(r_2-1)} e_2^{(r_2-1)} + \cdots + \alpha_{21} \dot{e}_2 \end{pmatrix} \\ &= \begin{pmatrix} y_{d1}^{(2)} + \alpha_{11} \dot{e}_1 \\ \dot{y}_{d2} \end{pmatrix} \triangleq m, \end{aligned} \tag{23}$$

and the coefficients α_{ij} are chosen so that the polynomial in m_i is Hurwitz. In this case, we can simply choose $\alpha_{11} = 1$. Choose control law as

$$u = G^{-1} \left[-F + m + K \cdot \operatorname{sgn}(S) \right], \tag{24}$$

where $\operatorname{sgn}(s_i)$ is the sigh function: $\operatorname{sgn}(s_i) = +1$ if $s_i > 0$, $\operatorname{sgn}(s_i) = 0$ if $s_i = 0$, $\operatorname{sgn}(s_i) = -1$ if $s_i < 0$, and $K = [k_1, k_2]^T$ with $k_1 > 0$ and $k_2 > 0$. By substituting (24) into (22), we get

$$\begin{aligned} \dot{s}_1 &= -k_1 \cdot \operatorname{sgn}(s_1), \\ \dot{s}_2 &= -k_2 \cdot \operatorname{sgn}(s_2), \end{aligned} \tag{25}$$

which means $\lim_{t\to\infty} s_1 = 0$ and $\lim_{t\to\infty} s_2 = 0$; thus s_i goes to zero in finite time. Once the trajectory reaches the sliding surfaces, it follows that $\lim_{t\to\infty} e_1 = 0$ and $\lim_{t\to\infty} e_2 = 0$. Therefore the tracking performance is achieved.

Choose Lyapunov function as $V = V_1 + V_2 = s_1^2 + s_2^2$. The time derivative of V is

$$\begin{aligned} \dot{V} &= \dot{V}_1 + \dot{V}_2 = s_1 \dot{s}_1 + s_2 \dot{s}_2 \\ &= -k_1 \cdot \operatorname{sgn}(s_1) - k_2 \cdot \operatorname{sgn}(s_2) \le 0. \end{aligned} \tag{26}$$

Therefore the stability of the system is guaranteed.

3.2. Compensating Time Delays. As illustrated in Figure 4, the time delays of valve actuator T_1 and flow sensor T_2 as well as the balanced delays T_1' and T_2' will affect system controllability; thus the delays should be compensated. The most common method to compensate time delays is Smith predictor [32]. The concept of Smith predictor is separating time delays from the system, controlling the delay-free part in an inner loop, and correcting modelling error and disturbance in an outer loop [33]. Since the inner control loop does not contain any time delays, the main controller can obtain a quick response to the system. The time delays of the bench or plant as a whole cannot be taken apart directly, so the model of the bench without time delays is needed for a quick response, which makes Smith predictor a model-based control method. However, the conventional Smith predictor is sensitive to modelling error of the system.

To overcome the dependence of modelling accuracy, a modified Smith predictor [34] is applied for the pump-valve system in Figure 4, as shown in Figure 5. Compared with conventional Smith predictor, the modified Smith predictor introduces a first-order filter to attenuate the oscillations of the error between the real system and the predicted one. Therefore it can tolerate larger modelling errors, reduce the dependence on model accuracy, and improve the robustness of the system [35]. The first-order filter can be chosen as (27). T_f can be chosen as half of the pure time delay [35]; $T_f = 0.5 \times (T_1 + T_2)$ for both outputs for the model equation (10) since the time delays are balanced.

$$G_f(s) = \frac{1}{T_f s + 1}. \tag{27}$$

Therefore the overall control flow chart can be modified as Figure 6.

4. Experiment Validation and Analysis

To validate the control method developed in this paper, the experiment is done on the test bench as shown in Figure 3(b). The PLC is chosen as ABB PM554; the upper computer software is Simulink on an Intel 2.3 GHz PC. The upper computer and PLC communicate via OPC protocol at a sample frequency of 1 Hz. Other parameters are chosen as $T_1 = 0.3$ s, $T_2 = 0.9$ s, $T_H = 1$ s, and $T_n = 0.4$ s based on the actual characteristics of the bench components. The control law is chosen as (24). The time constants of filters in (27) are chosen as $T_f = 0.5 \times (T_1 + T_2) = 0.6$ s.

The experiment result is shown in Figure 7. The set point trajectories are chosen as the outputs of the optimization algorithm in our previous work [10], which are two step signals. It is shown that the actual trajectories converge to the set point trajectories. A step disturbance triggered by decreasing the lift of the pneumatic valve representing pressure load ΔP_c from 60% to 40%, which is very common in industrial applications, is added to the system at $t = 300$ s. The disturbance caused a fluctuation in both ΔP and Q and the fluctuation is soon suppressed in 25 seconds. Therefore the controller is satisfying in tracking performance and antidisturbance performance.

To verify the cooperation of the optimization method in our previous work [10] and the control method in this paper on this one-pump system, a comparison of operation point deviation and power consumption between conventional speed regulation in [3] and the new method in this paper on a low pipeline resistance system at different flow rate requirements is simulated. The results are shown in Figures 8(a) and 8(b), respectively. The operation point deviation θ is defined as (28) [10]. The genetic algorithm is applied on the single pump system and its optimization result is used as the input of the controller. The conventional speed regulation does not regulate valve and only regulates the pump speed using a simple PID controller; therefore the operation point is always far away from BEP if the pump is oversized for

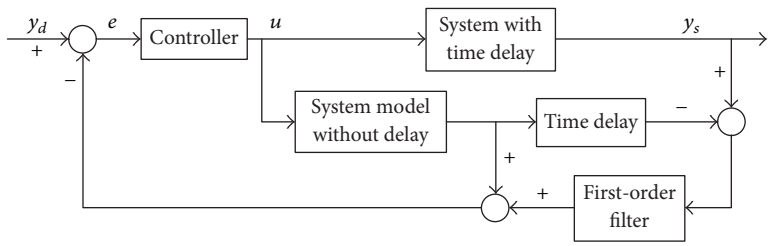

Figure 5: Schematic of modified Smith predictor.

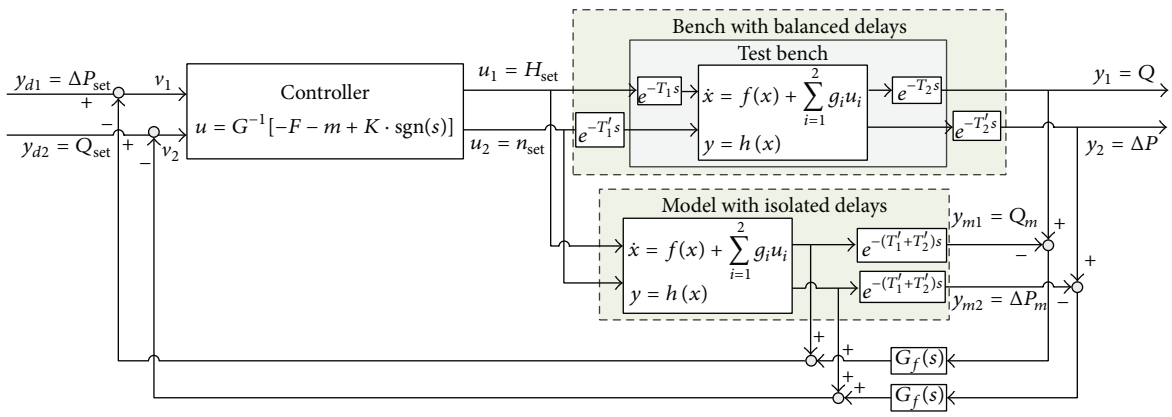

Figure 6: Overall control flow chart.

the system. Since the system in Figure 3(a) is a closed-loop test rig, the static head for the system curve is very small. In this case, the system curve is a parabolic curve similar to the BEP curve as pump speed varies. Figure 2 gives a qualitative explanation. For the initial operation point A, the BEP at operation speed n_0 is point F. When the operation point changes to point C using conventional speed regulation, the BEP becomes point E. However, the changes of BEP and operation point are almost equally proportional due to the similarity of the BEP curve and the system curve R_0. Therefore the deviation almost remains constant as the flow varies for the conventional speed regulation.

$$\theta = \frac{Q - Q_{\text{BEP}}}{Q_{\text{BEP}}}. \tag{28}$$

The new method combines the optimization in our previous work [10] and the controller in this paper, optimizing the operation point and regulating both speed and valve. The new method obtains a wide flow range ($15\,\text{m}^3/\text{h}\sim30\,\text{m}^3/\text{h}$) of small operation point deviation (≤20% from BEP). The deviations from the BEPs are clearly decreased at all flow rates for the new method; thus the reliability of the pump is improved. However, the power consumption is higher, due to extra energy consumed at part open control valve compared to conventional speed regulation method. In other words, the overall efficiency of the system is decreased for a better pump reliability. Better operation point cuts down the component failure rate and reduces maintenance cost, while lower system efficiency increases energy cost. If the benefits gained from better pump reliability win over the costs of higher power consumption, it is suitable to apply this strategy to obtain higher reliability. The method is applicable for situation that requires high reliability but is insensitive to power consumption. If the flow rate far exceeds the BEP, the valve consumes a large amount of energy to shrink the operation point deviation. When the energy cost increased exceeds the maintenance cost reduced, it becomes uneconomic for this one-pump system. In this case, it is suggested to substitute the pump to a smaller pump or apply pump number optimization in our previous work [10].

5. Conclusion

In this paper, a typical fluid conveying system that consists of one pump and one valve is built to study the control of balancing efficiency and reliability. A control strategy aimed at achieving the control of the pump-valve system based on the optimization result in our previous work [10] is developed. The pump-valve system is a time-delayed nonlinear MIMO system. In this paper, the time delays are isolated from the system to form a delay-free system and a time-delay component. A sliding mode controller is developed to control the delay-free system and the time delays of the system are compensated by a modified Smith predictor. The experiment results show that the controller achieves good tracking performance and robustness. This method takes full advantage of the existing imprecise system model and greatly decreases the complexity of the control algorithm compared to fuzzy adaptive method.

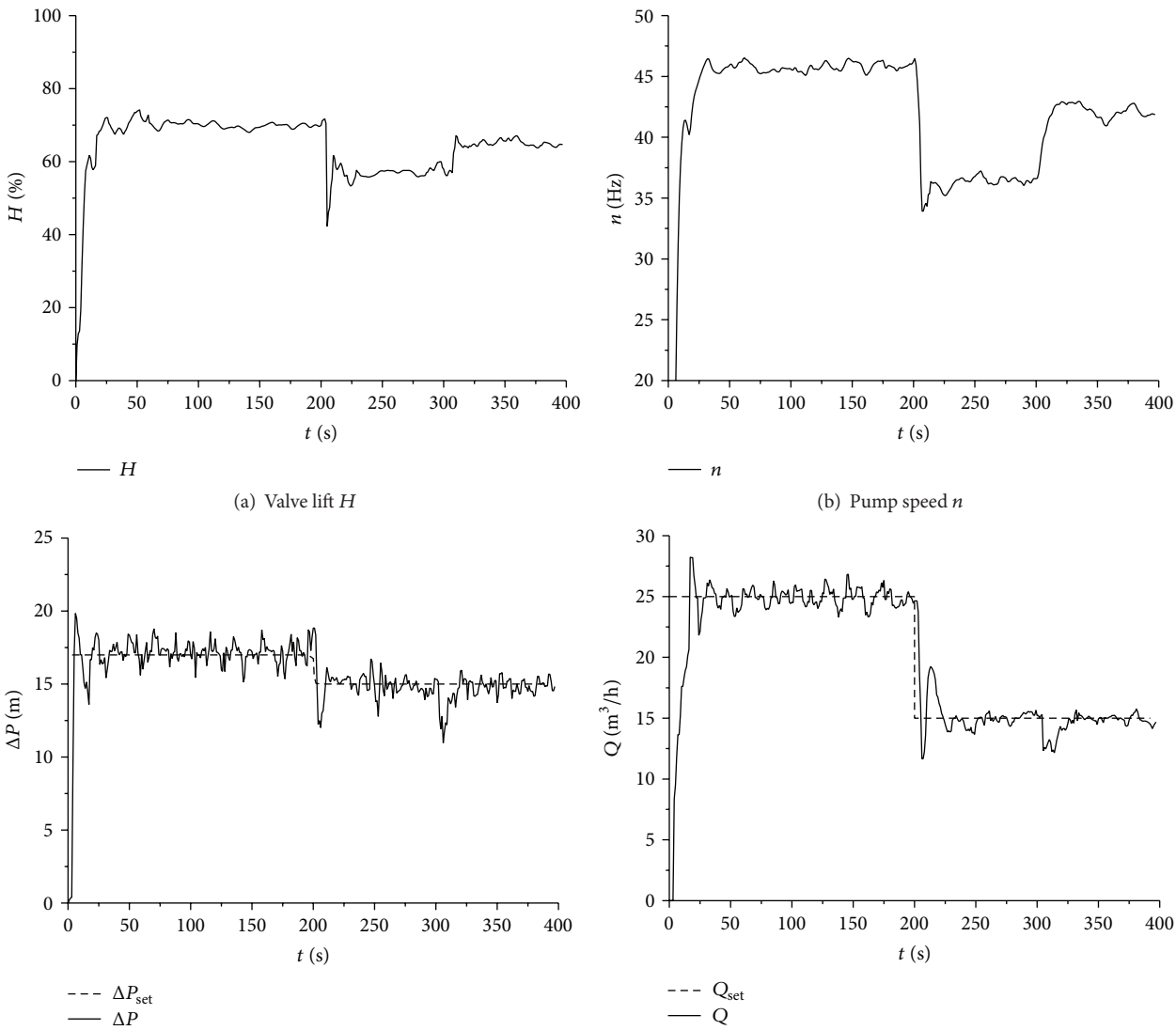

(a) Valve lift H

(b) Pump speed n

(c) Pressure losses ΔP_{set} and ΔP

(d) Flow rates Q_{set} and Q

Figure 7: Experiment results.

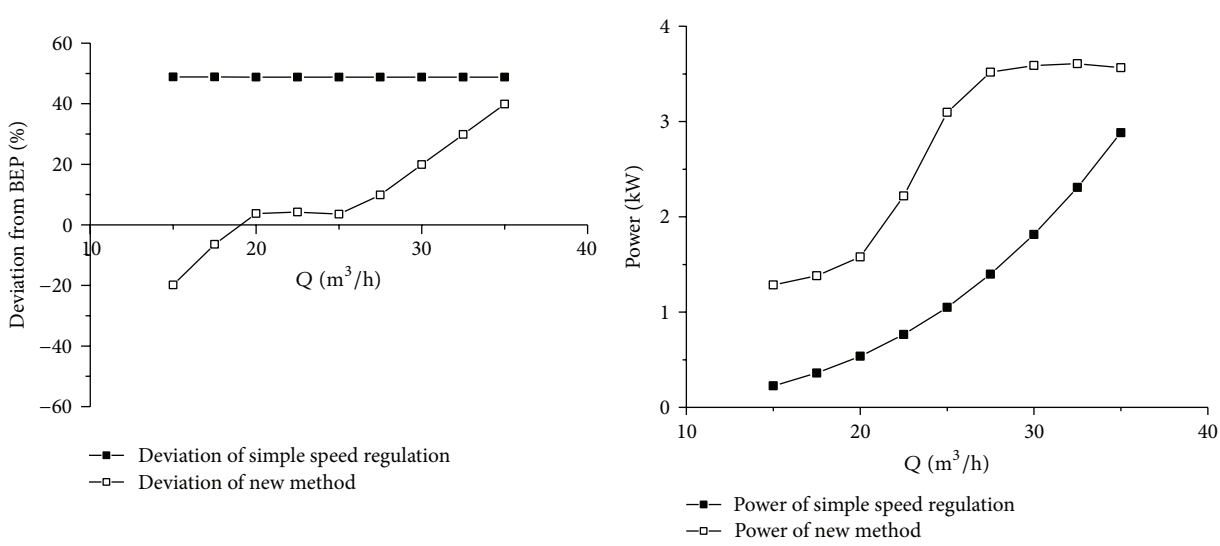

(a) Operation point deviation

(b) Power consumption

Figure 8: Comparison between conventional speed regulation and the new method.

A comparison of conventional speed regulation and the method combined with our previous work [10] is conducted. The comparison shows that the method can significantly reduce the operation point deviation at the cost of increasing power consumption. It is clearly shown in the comparison result that the new method sacrifices system efficiency for a better operation point. This paper offers an option to improve reliability of a class of fluid conveying systems, but it is worthwhile to weigh the better operation point against the higher energy consumption.

Competing Interests

The authors declare that they have no competing interests.

Acknowledgments

The authors would like to thank the support of National Natural Science Foundation of China (no. 51276213), Selected Postdoctoral Research Projects Foundation of Zhejiang Province (no. BSH1401015), and KSB AG.

References

[1] Freedonia, *Industry Report—Machinery Pumps in China. Industy Report*, Freedonia Group, Cleveland, Ohio, USA, 2011.

[2] L. Frenning, *Pump Life Cycle Costs: A Guide to LCC Analysis for Pumping Systems*, Hydraulic Institite & Europum & U.S. Department of Energys Office of Industrial Technologies, 2001.

[3] L. Jiang, Y. Chen, and G. Fan, "The design of constant pressure water supply system based on ABB inverter," *Procedia Engineering*, vol. 15, pp. 436–442, 2011.

[4] S. Paul and U.S. Department of Energy, *United States Industrial Electric Motor Systems Market Opportunities Assessment. Government Report*, Office of Energy Efficiency and Renewable Energy, Washington, DC, USA, 2002.

[5] M. Ciontu, D. Popescu, and M. Motocu, "Analysis of energy efficiency by replacing the throttle valve with variable speed drive condensate pump from E.C. Turceni," in *Proceedings of the 3rd International Symposium on Electrical and Electronics Engineering (ISEEE '10)*, pp. 293–297, IEEE, New York, NY, USA, September 2010.

[6] J.-Y. Wang, T.-P. Chang, and J.-S. Chen, "An enhanced genetic algorithm for bi-objective pump scheduling in water supply," *Expert Systems with Applications*, vol. 36, no. 7, pp. 10249–10258, 2009.

[7] S. S. Hashemi, M. Tabesh, and B. Ataeekia, "Ant-colony optimization of pumping schedule to minimize the energy cost using variable-speed pumps in water distribution networks," *Urban Water Journal*, vol. 11, no. 5, pp. 335–347, 2014.

[8] V. M. Cherkassky and B. Nikolaev, *Pumps Fans Compressors*, vol. 10, Mir, Moscow, Russia, 1980.

[9] H. P. Barringer, "How to use reliability engineering principles for business issues," in *Proceedings of the YPF Reliability Symposium*, La Platta, Argentina, November 1998.

[10] P. Wu, Z. Lai, D. Wu, and L. Wang, "Optimization research of parallel pump system for improving energy efficiency," *Journal of Water Resources Planning and Management*, vol. 141, no. 8, Article ID 04014094, 8 pages, 2015.

[11] F. J. T. E. Ferreira, J. A. C. Fong, and A. T. de Almeida, "Ecoanalysis of variable-speed drives for flow regulation in pumping systems," *IEEE Transactions on Industrial Electronics*, vol. 58, no. 6, pp. 2117–2125, 2011.

[12] A. Isidori, *Nonlinear Control Systems*, vol. 1 of *Communications and Control Engineering Series*, Springer, Berline, Germany, 3rd edition, 1995.

[13] S. Sastry, *Nonlinear Systems: Analysis, Stability, and Control*, vol. 10, Springer, New York, NY, USA, 2013.

[14] J. J. E. Slotine and W. Li, *Applied Nonlinear Control*, vol. 199, Prentice Hall, New Jersey, NJ, USA, 1991.

[15] C. Hwang, C. Lan, and W. Jieng, "The trajectory tracking of an electrohydraulic servo-mechanism via a sliding mode controller," *Proceedings of the Institution of Mechanical Engineers, Part I: Journal of Systems and Control Engineering*, vol. 207, no. 3, pp. 135–142, 1993.

[16] S. Wang, S. Habibi, and R. Burton, "Sliding mode control for an electrohydraulic actuator system with discontinuous non-linear friction," *Proceedings of the Institution of Mechanical Engineers, Part I: Journal of Systems and Control Engineering*, vol. 222, no. 8, pp. 799–815, 2008.

[17] V. I. Utkin, "Sliding mode control design principles and applications to electric drives," *IEEE Transactions on Industrial Electronics*, vol. 40, no. 1, pp. 23–36, 1993.

[18] G. Bartolini, A. Pisano, E. Punta, and E. Usai, "A survey of applications of second-order sliding mode control to mechanical systems," *International Journal of Control*, vol. 76, no. 9-10, pp. 875–892, 2003.

[19] Y. Feng, X. Yu, and Z. Man, "Non-singular terminal sliding mode control of rigid manipulators," *Automatica*, vol. 38, no. 12, pp. 2159–2167, 2002.

[20] T. Shaocheng, T. Jiantao, and W. Tao, "Fuzzy adaptive control of multivariable nonlinear systems," *Fuzzy Sets and Systems*, vol. 111, no. 2, pp. 153–167, 2000.

[21] W.-S. Lin and C.-S. Chen, "Robust adaptive sliding mode control using fuzzy modelling for a class of uncertain MIMO nonlinear systems," *IEE Proceedings: Control Theory and Applications*, vol. 149, no. 3, pp. 193–202, 2002.

[22] S. S. Ge and K. P. Tee, "Approximation-based control of nonlinear MIMO time-delay systems," *Automatica*, vol. 43, no. 1, pp. 31–43, 2007.

[23] B. Chen, X. P. Liu, K. F. Liu, and C. Lin, "Adaptive control for nonlinear MIMO time-delay systems based on fuzzy approximation," *Information Sciences*, vol. 222, pp. 576–592, 2013.

[24] V. Feliu-Batlle, R. Rivas Pérez, F. J. Castillo García, and L. Sanchez Rodriguez, "Smith predictor based robust fractional order control: application to water distribution in a main irrigation canal pool," *Journal of Process Control*, vol. 19, no. 3, pp. 506–519, 2009.

[25] M. Nasiri and M. Montazeri-Gh, "Time-delay compensation for actuator-based hardware-in-the-loop testing of a jet engine fuel control unit," *Proceedings of the Institution of Mechanical Engineers Part I: Journal of Systems and Control Engineering*, vol. 226, no. 10, pp. 1371–1380, 2012.

[26] J. M. Romero-García, J. L. Guzmán, J. C. Moreno, F. G. Acién, and J. M. Fernández-Sevilla, "Filtered Smith Predictor to control pH during enzymatic hydrolysis of microalgae to produce L-aminoacids concentrates," *Chemical Engineering Science*, vol. 82, pp. 121–131, 2012.

[27] G. Biswas, *Introduction to Fluid Mechanics and Fluid Machines*, McGraw-Hill Education, Columbus, Ohio, USA, 2nd edition, 2003.

[28] IEC-60534-2-1, Flow Equations for Sizing Control Valve, 2007.

[29] C. A. Smith and A. B. Corripio, *Principles and Practice of Automatic Process Control*, John Wiley & Sons, New York, NY, USA, 2nd edition, 1997.

[30] A. Hughes and B. Drury, *Electric Motors and Drives: Fundamentals, Types and Applications*, Newnes, Burlington, Mass, USA, 4th edition, 2013.

[31] V. G. Ivancevic and T. T. Ivancevic, *Geometrical Dynamics of Complex Systems: A Unified Modelling Approach to Physics, Control, Biomechanics, Neurodynamics and Psycho-Socioeconomical Dynamics*, vol. 31, Springer, Dordrecht, Netherlands, 2006.

[32] M. Rao and H. Qiu, *Process Control Engineering: A Textbook for Chemical, Mechanical, and Electrical Engineering*, vol. 1, Gordon and Breach Science, New York, NY, USA, 1993.

[33] O. J. Smith, "A controller to overcome dead time," *ISA Journal*, vol. 6, no. 2, pp. 28–33, 1959.

[34] C. Hang and F. Wong, "Modified smith predictors for the control of processes with dead time," in *Proceedings of the ISA Annual Conference*, pp. 33–44, Chicago, Ill, USA, October 1979.

[35] J. E. Normey-Rico, *Control of Dead-Time Processes*, Advanced Textbooks in Control and Signal Processing, Springer, London, UK, 2007.